# Approximation of mechanical properties of sintered materials with discrete element method

*Maksym* Dosta[1,*], *Robert* Besler[2], *Christian* Ziehdorn[1], *Rolf* Janßen[2], *Stefan* Heinrich[1]

[1]Institute of Solids Process Engineering and Particle Technology, Hamburg University of Technology, 21073 Hamburg, Germany

[2]Institute of Advanced Ceramics, Hamburg University of Technology, 21073 Hamburg, Germany

**Abstract.** Sintering process is a key step in ceramic processing, which has strong influence on quality of final product. The final shape, microstructure and mechanical properties, e.g. density, heat conductivity, strength and hardness are depending on the sintering process. In order to characterize mechanical properties of sintered materials, in this contribution we present a microscale modelling approach. This approach consists of three different stages: simulation of the sintering process, transition to final structure and modelling of mechanical behaviour of sintered material with discrete element method (DEM). To validate the proposed simulation approach and to investigate products with varied internal structures alumina powder has been experimentally sintered at different temperatures. The comparison has shown that simulation results are in a very good agreement with experimental data and that the novel strategy can be effectively used for modelling of sintering process.

## 1 Introduction

The sintering process is one of the most widely used heat treatment processes in the ceramic industry. During sintering densification of heated green body occurs and the free enthalpy, as well as, the surface and contact energies are minimized [1]. However, despite the wide applications of sintering process, until now there are no precise methods allowing to describe the process with high detailing grade. Nowadays, most of applied models are based on the continuum mechanical approach, where the material microstructure, anisotropy or high porosity cannot be effectively modeled [2].

In this contribution the application of the discrete element method (DEM) for modeling of sintering process is proposed. The DEM was initially formulated and applied to predict behavior of granular materials consisting of ideally spherical particles. However, in the recent years this method was extended with new contact models and calculations algorithms. One of the interaction laws was specially developed for modeling of material densification occurring during sintering process [3]. The main advantage of the DEM compared to experimental investigations is the detailed comprehensive information about trajectories and position of individual particles as well as forces acting on them. As an example Parhami and McMeeking [3] have proposed DEM model for description of initial stage sintering. This model was afterwards effectively applied by Martin et al. [4] for modelling of defects evolution. Based on this model Besler et al. [5] have investigated structural deformation of periodic macro porous alumina as well as densification of ceramic-metal composite materials with varying metal content [6].

Another extension of the DEM is a bonded particle model (BPM). By the BPM each two primary particles can be connected with solid or liquid bonds. Similarly to primary particles, all bonds are treated as separate objects. This allows to represent complex material structures with high porosities and to investigate their mechanical behaviour [7]. For example Kozhar et al. [8] have investigated breakage behaviour of micrometer-sized titania at compression with the BPM, Dosta et al. [9] applied this approach to predict strength of glass agglomerates.

In this contribution both extensions of the DEM which have been described above have been used for approximation of mechanical properties of sintered materials. For this purpose novel simulation strategy consisting of three stages has been proposed:

- first stage: modelling of the sintering process, where material densification is calculated using DEM;
- second stage: transition from a set of overlapped spheres to the bonded-particle model, consisting of non-overlapped spheres connected with solid bonds;
- third stage: investigation of mechanical material properties during three-points bending tests.

In this study, alumina powder ($Al_2O_3$) has been used as model material. Due to various chemical and physical properties, the processing of alumina has a set of advantages compared to other materials; therefore it is widely used for sintering.

* Corresponding author: dosta@tuhh.de

## 2 Experimental measurements

In order to validate model a set of experiments was performed to measure the mechanical properties of sintered material. In the first step, the green body was produced by material densification through uniaxial compression. For this purpose the press Model 10 of company Paul-Otto Weber GmbH with matrix dimensions of 470 x 45 x 620 mm was used.
Afterwards, the sample was pressed again through cold isostatic pressing with a pressure of 150 MPa. The resulting green body was analyzed in order to obtain information about its composition (e.g. density, dimensions).
Thereafter, all samples were sintered by varying temperatures between 1100 °C and 1250 °C in the chamber oven HT 04/17 of company Nabertherm GmbH. In the case of all studies the heating up and cooling down process was controlled by a temperature increase and decrease of 10 $K \cdot min^{-1}$. The holdup time for each sintering temperature was equal to one hour.
Directly after the sintering process, all samples were measured again to obtain information about their new geometrical characteristics and density. In Fig. 1 dependency between sintering temperature and relative density is illustrated.

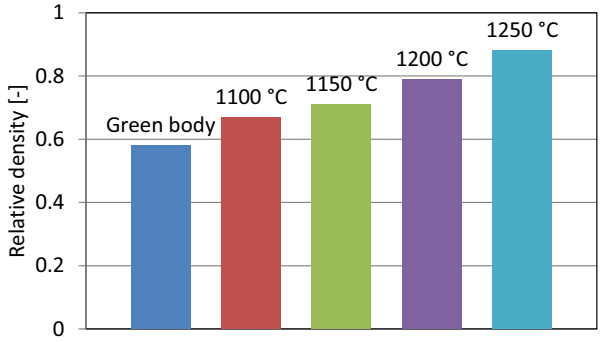


**Fig. 1.** Dependency of samples densities from sintering temperature.

Before proceeding with the bending tests, each specimen was polished coplanar to ensure the correct measurement of Young's modulus. All bending tests were accomplished by the three point bending process in a self-developed bending device at the Institute of Advanced Ceramics of Hamburg University of Technology. In order to minimize position effects, each specimen was loaded and unloaded for three times with a maximum loading force of 60 N. To receive the value of the slope of the force-displacement characteristic, only the last discharge cycle with values between 50 N and 20 N was taken into account.

## 3 Modelling of sintering process

For the modeling of sintering process the contact model proposed by Parhami and McMeeking [3] was implemented into the component-based simulation framework MUSEN [10]. According to this model, between each two contacting particles, the forces in normal and tangential direction are acting. The normal force is described with Eq. 1 and consists of two terms:

- viscous force, which describes resistance against relative motion;
- sintering force acting toward the contacting particles.

$$F_n = \pi v_{rel} a^4/(2\beta\Delta_b) - \alpha\pi R\gamma/\beta \quad (1)$$

where $v_{rel}$ is a relative velocity, a is a contact radius, α and β are parameters which define ratio between grain boundary to surface diffusion, R is a particle radius, $\Delta_b$ diffusion parameter.

The force in tangential direction depends on the relative velocity in tangential direction, the dimensionless coefficient of friction and the contact radius between two particles. Detailed description of the model and its application on alumina or on ceramic-metal composites can be found in Besler et al. [5], [6].

The main parameters which have been used for DEM simulation of sintering process are listed in Table 1. In order to decrease calculation time a scaling factor has been introduced. With help of scaling factor the mass of primary particles has been increased. Such scaling allow to increase calculation time step and as a consequence to decrease calculation time.

**Table 1.** Main simulation parameters.

| Parameter | Value |
|---|---|
| Density [$kg/m^3$] | 3950 |
| Particle diameter [nm] | 100 |
| Surface energy [$J/m^2$] | 1.1 |
| Atomic volume [$m^3$] | 8.47e-30 |
| Particles number | 99000 |
| Scaling factor | 1e+20 |

Contrary to the experiments, the simulation of sintering has been performed only for one specific value of temperature 1200 °C. As result, the time-dependent change of the relative density in the sample has been obtained. In Fig. 2 time-dependent propagation of the relative density is shown with solid line. It can be seen that with an increased sintering time the density increased from 0.58 (green body) up to 0.9.

In order to get direct correlation between simulation and experimental data four time points with porosities equal

to the experimental obtained data (0.67, 0.71, 0.79, 0.88) have been selected. These time points have been used afterwards as initial data for the second modeling stage.

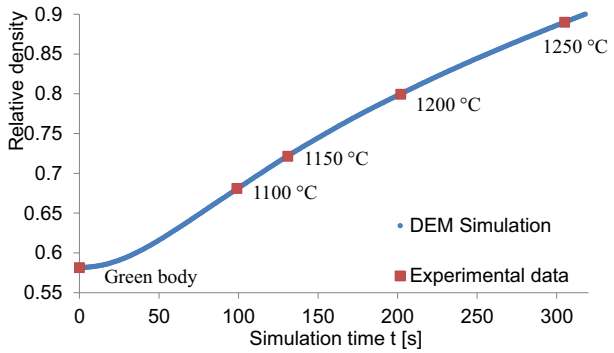


**Fig. 2.** Time-dependent propagation of relative density.

## 4 Transition to BPM

After modeling of sintering process the alumina sample was represented as a set of overlapped ideally spherical particles. In order to perform further calculations of the mechanical properties, the transition to the bonded-particle model has been done. During this transition, each two overlapped primary particles have been converted into the system of smaller non-overlapped spherical particles with cylindrical solid bond between them, as it is schematically illustrated in Fig. 3.

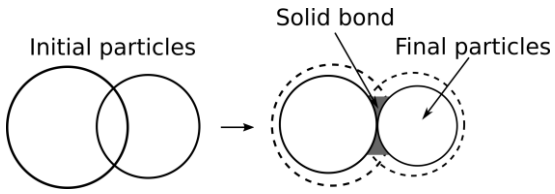


**Fig. 3** Schematic representation of transition algorithm.

The transformation was performed as an iterative process. In the every iteration of algorithm, all pairs of the overlapped particles in the sample were identified. Afterwards, radii of overlapped particles $R_n$, $R_m$ in each pair were decreased according to:

$$R_{n,i+1}=R_{n,i}-\Delta R;\ R_{m,i+1}=R_{m,i}-\Delta R \quad (2)$$

where $i$ is the number of iteration and $\Delta R$ is the decrement which was equal to 0.0001 nm. To fulfill mass conservation, the volume of the corresponding solid bond between particles $n$ and $m$ ($V_{nm}$) was increased according to Eq. 3. Iterations have been repeated until there is no more pair of overlapped particles in the system.

$$V_{nm,i+1} = V_{nm,i}+4/3\pi(R^3_{m,i}+ R^3_{m,i} -R^3_{m,i+1}- R^3_{n,i+1}) \quad (3)$$

When the algorithm was finished the radii and lengths of all bonds were calculated based on their volumes. During calculation it was considered, that the length of the bond $L_b$ between two particles with radii $R_1$ and $R_2$ is equal to:

$$L_b = L_{pp}-(R_1^2-R_b^2)^{0.5}-(R_2^2-R_b^2), \quad (4)$$

where $L_{pp}$ is distance between particle centres and $R_b$ is bond radius. In Fig. 4 the size distribution of bonds radii obtained for sintering temperature 1100 (porosity 0.67) is shown.

In Table 2 main properties of bonds for different case studies are listed. It can be seen, that increase of the sintering temperature leads to the significant increase of the solid bonds number. This is caused due to sample shrinkage and formation of new interparticulate contacts.

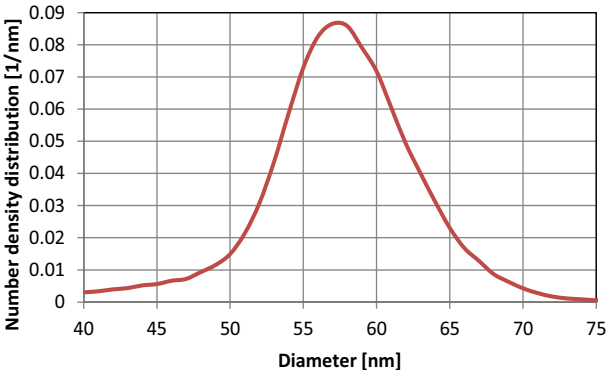


**Fig. 4** Distribution of solid bonds according to their radii.

**Table 2.** Parameters of solid bonds.

| Parameter | 1100 °C | 1150 °C | 1200 °C | 1250 °C |
|---|---|---|---|---|
| Average diameter [nm] | 57.2 | 56.89 | 56.26 | 55.56 |
| Average length [nm] | 23.9 | 24.5 | 25.46 | 26.51 |
| Bonds number [-] | 270514 | 288655 | 321888 | 353318 |

## 5 Approximation of mechanical properties

In the final stage mechanical properties of material has been modeled with DEM. For this purpose three-point bending test has been used. Sample was placed between three cylindrical punches and upper cylinder was moved downwards with predefined velocity. For particle-particle or particle-wall interactions Hertz-Mindlin contact model was used. The solid bonds have been calculated according to the model of elastic solid beam [9].

Young's modulus and Poisson ratio of primary particles and bonds were equal to 400 GPa and 0.23. These are the parameters of alumina material which was used in the experimental measurements.

In Fig. 5 simulation results for one case study are shown. In this figure particles are hided and only solid bonds are shown. The bonds are colored according to the distribution of forces acting in them. It can be seen that in the upper part of sample mainly compression forces are acting on bonds and in the lower part the tension forces.

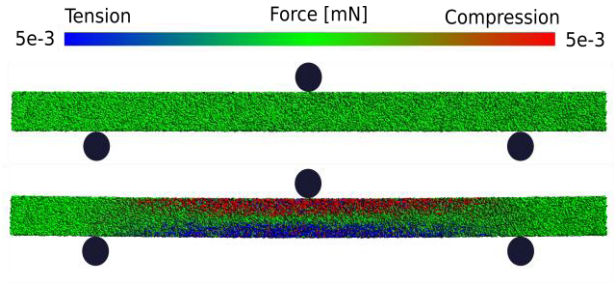


**Fig. 5.** Forces acting in solid bonds during three-points bending test.

Based on the simulation results the Young's moduli of the final samples have been approximated. This has been done based on the analysis of the obtained force-displacement characteristics. The numerically and experimentally obtained dependencies between sample porosity and Young's modulus are shown in Fig. 6. In the same figure the correlation proposed by Knudsen [11] is illustrated.
From the analysis of obtained results the conclusion can be drawn that proposed model is in a relative good agreement with the experimental results and is able to predict the stiffness of the sintered material for the relative densities in the range between 0.7 and 0.9. However, it should be mentioned, that the DEM model for calculation of sintering process does not contain terms which are able to describe grain growth. As a consequence this model cannot be applied for densities larger than 0.9.

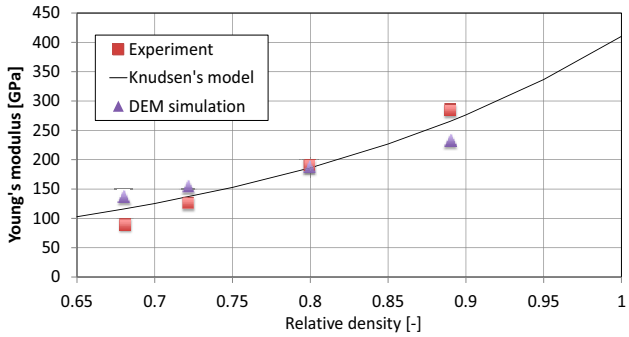


**Fig. 6.** Dependency of the Young's modulus on the relative density of sintered material.

## 6 Conclusion

In this contribution the microscale modeling approach to predict stiffness of sintered materials has been proposed. This approach based on the discrete element method and bonded-particle model and allows to investigate properties of sintered material. However, the developed model can be effectively applied only for relative porosities in the range between 0.7 and 0.9. In the further investigations it is planned to extend sintering model with terms to describe grain growth.

## Acknowledgments

We gratefully acknowledge financial support from the German Research Foundation (DFG) via SFB 986 "M3", project A3 and C5.

## References

1. H. Salmang, H. Scholze, R. Telle. *Keramik* (Springer Verl., 2007).
2. E.A. Olevsky. Mat. Sci. Eng. R. **2**, 41-100, (1998).
3. F. Parhami, R. McMeeking, Mech. Mat. **2**, 111-124 (1998).
4. C.L. Martin, H. Camacho-Montes, L. Olmos, D. Bouvard, R.K. Bordia, J. Am. Ceram. Soc. **7**, 1435-1441 (2009).
5. R. Besler, M. Rossetti, M. Dosta, S. Heinrich, R. Janssen, J. of the Amer. Ceram. Soc., **26**, 1021-1030 (2015).
6. R. Besler, M.R. da Silva, M. Dosta, S. Heinrich, R. Janssen, J. of the Europ. Ceram. Soc. **36**, 2245-2253 (2016).
7. D.O. Potyondy. Geosystem Eng. **18**, 1-28, 2015.
8. S. Kozhar, M. Dosta, S. Antonyuk, S. Heinrich, L. Gilson, U. Bröckel. Adv. Powd. Techn. **26**, 767-777 (2015).
9. M. Dosta, S. Dale, C.R. Wassgren, S. Heinrich, J.D. Litster, Powd. Techn. **299**, 87-97 (2016).
10. M. Dosta, S. Antonyuk, S. Heinrich. Ind. Eng. Chem. Research **52**, 11275-11281 (2013).
11. F.P. Knudsen, Journ. of Amer. Ceram. Soc. 45, 94-95, (1967).